LB - 827

A HIGH-VOLTAGE COLD-CATHODE RECTIFIER

RADIO CORPORATION OF AMERICA
RCA LABORATORIES DIVISION
INDUSTRY SERVICE LABORATORY

RADIO CORPORATION OF AMERICA

RCA LABORATORIES DIVISION

INDUSTRY SERVICE LABORATORY

LB-827

A High-Voltage Cold-Cathode Rectifier

Approved

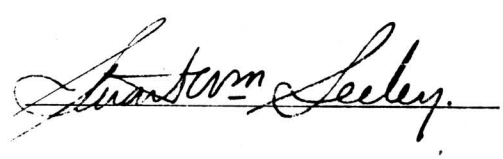

SUMMARY

The purpose of this investigation was to develop a rectifier tube, utilizing the principle of electron trapping in a magnetic field, for applications such as a high-voltage, television receiver supply.

The tube developed in this investigation has characteristics which compare favorably with the high-vacuum, thermionic rectifier 1B3GT, but has the added advantage of requiring no heater supply. The project has resulted also in the experimental determination of the criteria for rectification in structures that will maintain a low-pressure discharge in an electric and magnetic field. The new design was found superior to previous types of tubes of this sort, with respect to peak inverse voltage, dc characteristics and ac characteristics. This tube appears to offer, for the first time, a practical cold-cathode rectifier for voltages up to 10 kv, and currents up to 1 ma.

A High-Voltage Cold-Cathode Rectifier

Introduction

This bulletin deals with a cold-cathode, high-voltage, rectifier tube, which was developed as a part of a project on electron trapping devices. The general principle of electron trapping is herein discussed, as involved in the operation of the new tube. This is a type of trapping which is produced by the combined action of electric and magnetic fields. It results in an electrical discharge resembling a glow discharge, but differing in that a magnetic field is required to maintain it.

General Discussion

The history of gas discharges in electric and magnetic fields goes back to 1898, when such a discharge was observed by C.E.S. Phillips.[1,2] On that occasion, Phillips had reduced the pressure in a vessel sufficiently low to extinguish a glow discharge between two electrodes and then switched on a magnetic field along the axis of the two electrodes. A mysterious, luminous ring was observed to form between the electrodes and the glass wall, as indicated in Fig. 1. This glow was interpreted by R.J. Strutt[3] in 1913, as being due to ionization of the gas in the vessel, by negative ions traversing long paths, on going transverse to the magnetic field, from the two center electrodes to the glass wall, which had been charged positive by the previous discharge. To check this explanation, Strutt placed a cylindrical electrode close to the inside of the glass wall and concentric with the center electrodes. When this outer electrode was held at certain positive potentials, a discharge was maintained, under certain magnetic field strengths, between this electrode and the center electrodes, which were at ground potential. A conducting cylindrical jacket over the two center electrodes, as shown in Fig. 2, gave the same result. The effect was then investigated by several other workers,[4] and was later applied as a commercial rectifier by V. Bush and C.G. Smith.[5]

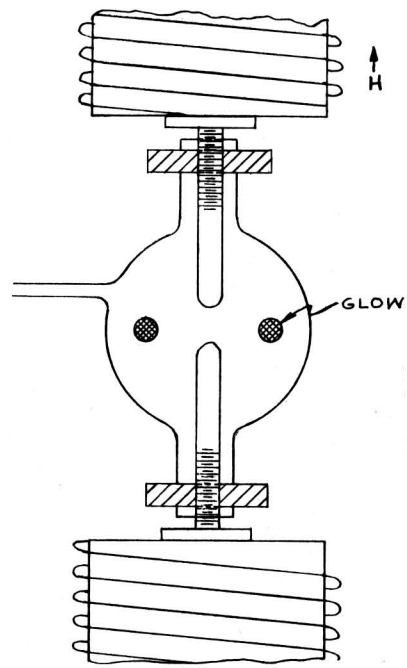

Fig. 1 – Apparatus used by C.E.S. Phillips to study glow discharge in magnetic field.

Bush and Smith used the structure of Strutt, shown in Fig. 2, with a magnetic field adjusted too low for conduction, when the center cylinder was the cathode, but sufficiently high for conduction, when the outer

cylinder was the cathode. These characteristics are illustrated in Fig. 3. The difference in magnetic field required by the different polarities was explained on the basis of Hull's[9] magnetron equations as being due to the smaller magnetic field required for cutoff in the inverted magnetron (outer cathode) compared to the same structure as a magnetron (inner cathode). This design was found to have appreciable back current above a few thousand volts, and was replaced by the thermionic gas rectifier, which was more reliable with the same inverse voltage rating. An application of the effect, which is still in use, was made by F.M. Penning[7,8] as an ionization gauge.

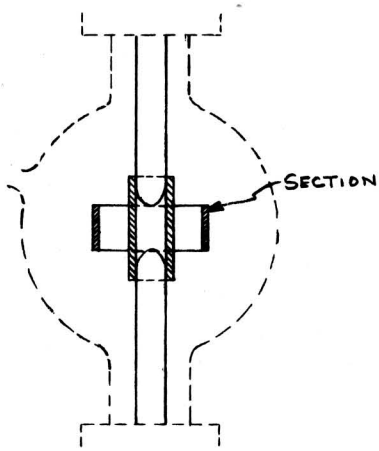

Fig. 2 – Strutt's modification of the apparatus of Fig. 1.

Penning first made an analysis of the known cutoff curves (Fig. 3) by applying Hull's equations to the case of electrons originating throughout the space between the electrodes. Using this procedure he calculated the ranges of voltages and magnetic fields under which electrons could pick up enough energy for ionization. These calculations qualitatively fit the observed data of cutoff. No attempt was made to determine time-variable characteristics, either theoretically or experimentally. After the cutoff analysis, Penning used the structure of Strutt[3] (Fig. 2 without the center sleeve) as a pressure gauge. Some further use[9] of the effect was made in 1946 by switching on the magnetic field to obtain conduction for a magnetron pulser.

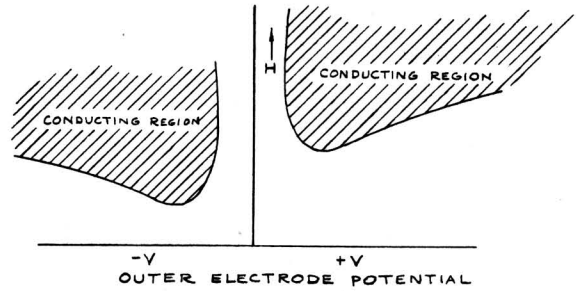

Fig. 3 – Static characteristics of a glow discharge between coaxial cylinders in the presence of a magnetic field.

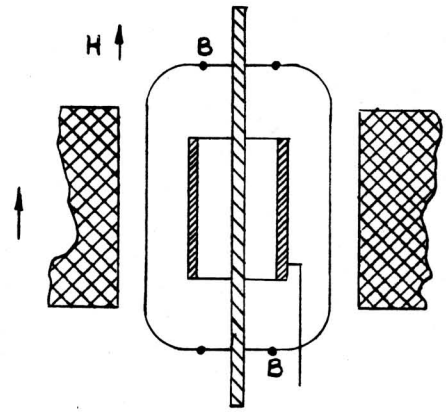

Fig. 4 – Diagram of apparatus first used.

Structures similar to that of Bush and Smith have been tested and found unable to withstand high inverse voltages. The tubes which have been developed in this laboratory employ radically improved electron trapping, thereby permitting very low gas pressures and the ability to withstand high voltages. A systematic investigation of the various geometrical electrode arrangements, described below, resulted in a final design in which the cathode is located in the center and has end plates. At the same time that it possesses improved conduction in one direction, due to improved trapping, it has also the ability to withstand very high inverse voltages. This tube differs basically from the tube of Bush and Smith in that it conducts in the opposite direction, i.e., from the center outward.

Theory of Operation

The formulation of a complete theory of the operation of this tube has not as yet been

carried out because of mathematical difficulties in meeting the exact boundary conditions. For example, the electron paths are dependent upon complicated electric and magnetic field distributions, also upon space charge, and collisions with molecules and ions. However, a quite useful idea of the operation of this type of tube can be gained from a simplified theory in which the actual structure is replaced by one of more amenable geometry. This has been done in the following discussion. Although the results do not admit of a quantitative check by experiment on all points, yet the qualitative agreement is good. The theory has been very helpful in the understanding and development of the tube.

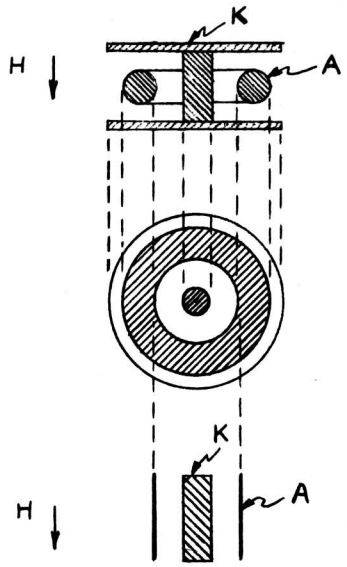

Fig. 5a – Electrode geometry of the tube.

Fig. 5b– Simplified representation.

The electrode geometry is shown schematically in Fig. 5a, and in detail in Figs. 32 and 33. The tube consists of a spool-shaped cathode K, and a ring-shaped anode A*, immersed in an axial magnetic field H. For the purpose of analysis this is here replaced by the concentric cylinder arrangement shown in Fig. 5b. The latter arrangement constitutes a cylindrical magnetron type of device, for which the theory of orbits has already been well developed by numerous authors. These results are now directly applicable to the present case.

Electrons leaving cathode K (Fig. 5b), travel in radial paths to anode A, in the absence of a magnetic field. However, if a field is present, these paths become curved, and at a critical field H_c, the curvature is so great that they fail to reach the anode and return towards the cathode. The same is true of electrons originating at any point in the interelectrode space, providing that the magnetic field is sufficiently large. Referring to Fig. 6, an electron originating at P, a distance r_1, from the center, will traverse a path such as shown, for fields such that $H>H_c$.

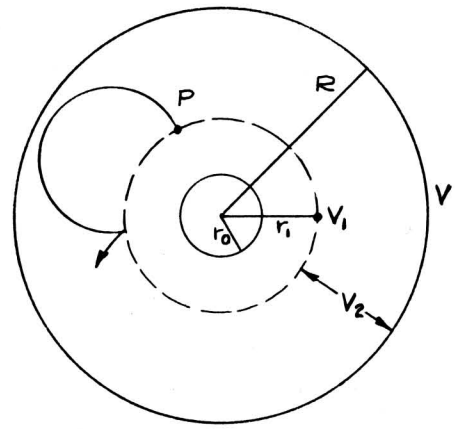

Fig. 6 – Diagram showing quantities affecting electron trajectories.

From Hull's[a] magnetron theory H_c is given by

$$H_c = \sqrt{\frac{8m\,V_2}{e}}\ \frac{R}{R^2-r_1^2} \qquad (1)$$

where the quantities are defined in Fig. 6. This will be modified by introducing an expression for V_2. Normally, in a concentric cylinder arrangement, the potential varies logarithmically between the cylinders, however, in the present case, due to the presence of the cathode end plates, this potential variation becomes more linear. Hence it will be assumed that

$$V_2 = V\,\frac{R-r_1}{R-r_0}.$$

Using this expression, and also letting the cutoff field for $r_1=r_0$ be H_{co}, yields

$$\left(\frac{H_c}{H_{co}}\right)^2 = \frac{\left(1+\frac{r_0}{R}\right)^2\left(1-\frac{r_0}{R}\right)}{\left(1+\frac{r_1}{R}\right)^2\left(1-\frac{r_1}{R}\right)} \qquad (2)$$

*Strictly speaking these electrodes are not cathode and anode in the usual sense, but function as such during the period of conduction.

This result is plotted in Fig. 7, for the case where $r_o/R = 0.25$. This graph shows that if $H_c = H_{co}$, all electrons originating between the cathode surface, $r = 0.25R$, and the surface $r = 0.45R$, are cut off, and fail to reach the anode, as shown in Fig. 8a. If $H_c = 2H_{co}$, the cutoff region extends from the cathode to about $r = 0.92R$, as shown in Fig. 8b. An electron originating at $r = 0.92R$ will just graze the anode, as shown at a. An electron originating in the central region ($r \approx R/2$), will have an orbit such as shown at b.

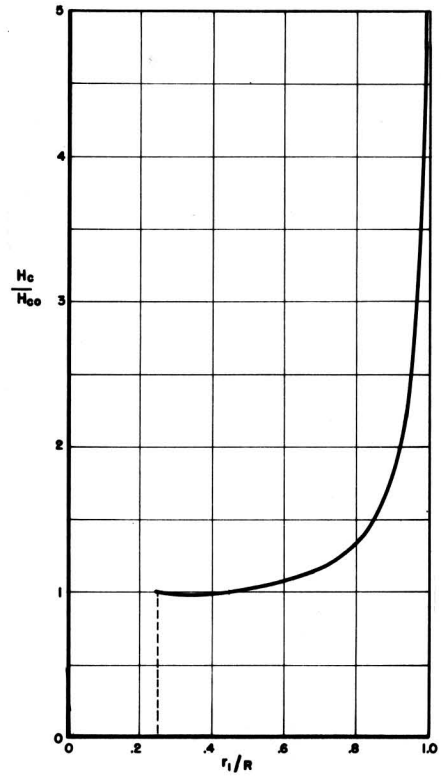

Fig. 7 – Electron cutoff as a function of point of origin.

The above orbits are drawn to represent those with zero initial velocity. Small initial velocities, such as may exist after an ionization process in gas discharge, in the voltage range involved here, affect the detailed curvelinear nature of the orbit, but not its general size and position. Fig. 8c shows the effects of small initial velocities: (a) $v_o = 0$; (b) v_o, radial; and (c) v_o, tangential.

The orbits of Fig. 8 are those of the simple cylindrical arrangement of Fig. 5b. In the structure of Fig. 5a they become more complicated, in that motion in the axial direction also occurs.

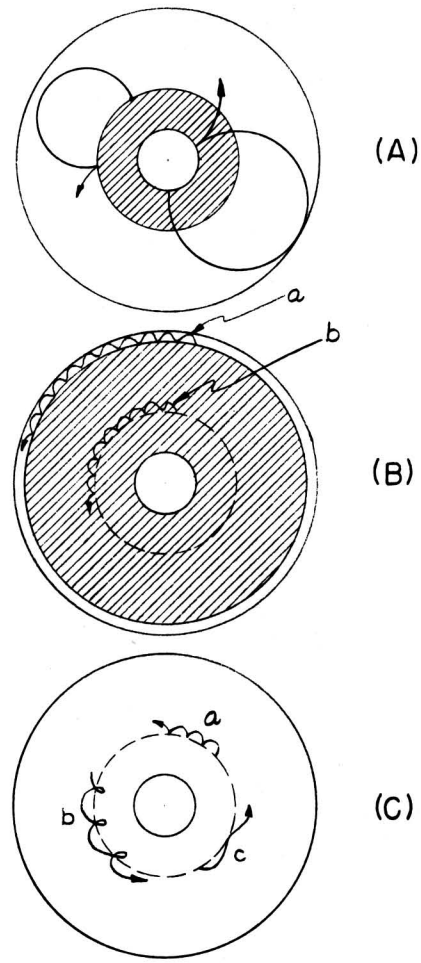

Fig. 8 – Typical electron paths from cylindrical case.

In Fig. 9 side views of the tube are included. The case where the electron originates in the equatorial plane is shown at 9a. Here the orbit is planar, and as already shown in Fig. 8. If the electron originates off the equatorial plane it will have an axial component of motion. This will be oscillatory, back and forth through the equatorial plane, since the electron will be attracted by the anode and repelled by the end plates. This oscillatory motion will be accompanied by a curvelinear azimuthal motion as shown in Fig. 9b.

The situation is considerably different when the anode is negative. The equatorial electrons then move as shown in Fig. 9c. The nonequatorial electrons move in short spiral paths to the end plates, where they are collected, as shown at (D).

These orbits illustrate the principle of "electron trapping", For example, in the orbits

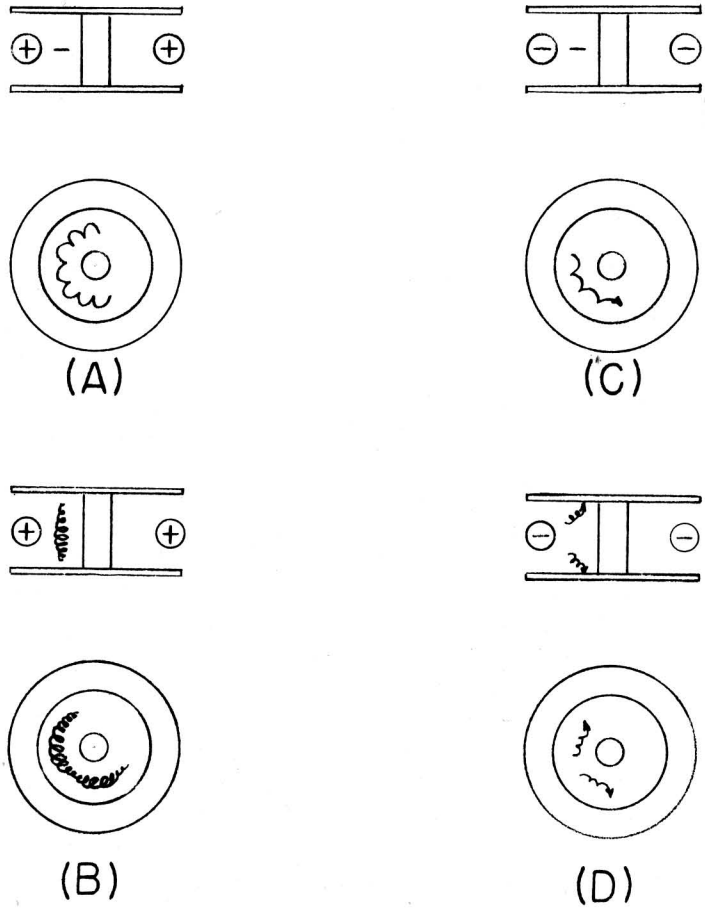

Fig. 9 – Typical electron paths for the tube.

of Fig. 9a and 9b, the electrons are unable to reach any electrode. The magnetic field curves their paths in such a way that no electrons reach the anode. The cathode exerts a repelling effect since its potential is negative with respect to the point of origin of the electron. Hence all such electrons are trapped. They remain in the interelectrode space until disturbances, such as collisions, deflect them into new paths, and eventually to the anode.

When the anode is negative this trapping effect is greatly reduced. The paths are then as shown in Fig. 9c and 9d. The equatorial electrons are trapped, as at 9c, but the non-equatorial ones, which actually constitute almost the entire number, move in short paths directly to the cathode, as shown at 9d.

Hence, when the anodes are positive there is a pronounced trapping effect, so that a high density of long-path electrons is built up. Whereas if the anode is negative, the electrons are quickly removed, the density is low and the path length short. These conditions greatly affect the conduction through the tube, and one responsible for its rectifying action.

The relation of the trapping effect to conduction may be explained by use of the Townsend theory of conduction in gases. Briefly, this theory assumes that electrons emitted from the cathode build up an electron avalanche by a process of cumulative ionization. Positive ions, formed in this process, return to the cathode and cause new electrons to be emitted. This is a feed-back phenomenon. Under the proper conditions the feedback may be large enough so that a continuous, self-sustaining discharge is formed.

The current i in a Townsend discharge is related to the primary current i_o at the cathode by the relation

$$m = \frac{i}{i_o} = \frac{\varepsilon^{\alpha x}}{1 - \gamma\,(\varepsilon^{\alpha x} - 1)} \qquad (3)$$

where α is the average number of electrons, or ions, formed per centimeter of path per electron, γ is the number electrons emitted from the cathode per positive ion striking its surface, and x is the electron path length between cathode and anode. It is evident that for certain values of αx and γ, m will be infinite. This corresponds to the onset of a self-sustaining discharge. The values of γ required at different values of αx to make m infinite, and the discharge self-sustaining, are plotted in Fig. 10.

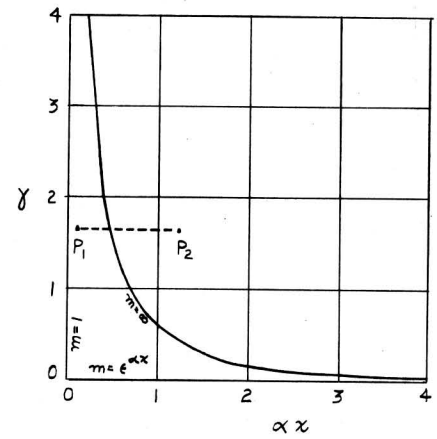

Fig. 10 – Conditions determining start of discharge.

From this figure it is seen that at point P_1 a self-sustaining discharge will not occur. This point might correspond to operation with the anode negative, since x is then small.

However, if the anode is positive, electron trapping occurs, and x becomes large, corresponding to point P_2. A self-sustaining discharge will then start since conditions are such that the boundary m = ∞ is crossed. The tube will act as a rectifier whenever P_1 and P_2 are on opposite sides of this boundary.

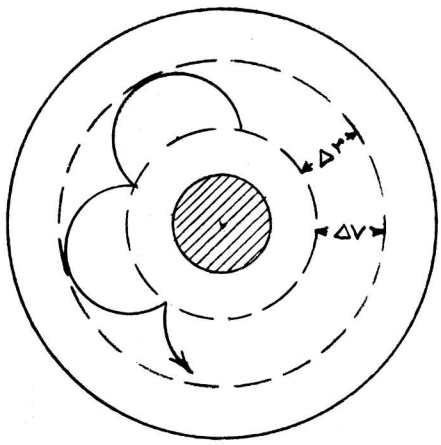

Fig. 11 – Diagram showing maximum energy gain Δv of electron moving over a range Δr.

It is clear that the shape of the orbit affects the length of the electron path or the value of x. The orbit also affects the value of α as illustrated in Fig. 11, by setting the limits of the potential difference through which the electrons are accelerated or decelerated. Assuming that the initial velocity of the electron is negligible, the maximum energy that it may have in the illustrated orbit is ΔV_e. A necessary condition for the formation of a discharge is that ΔV exceed the ionization potential. The amount of this excess is determined by the value of α required to satisfy the Townsend condition and yield a value of m = ∞.

As before, assuming a linear potential distribution between cathode and anode, the following relations are valid

$$\frac{R}{\Delta r} = \frac{V}{\Delta V}, \tag{4}$$

$$E = \frac{V}{R} = \frac{\Delta V}{\Delta r}. \tag{5}$$

From the equation of electron motion[9],

$$\Delta r = \frac{2m\ E}{H^2 e}. \tag{6}$$

From Eqs. (5) and (6)

$$H^2 = \frac{2m}{eR}\frac{V}{\Delta r},$$

and using Eq. (4)

$$H^2 = \frac{2m}{eR^2}\frac{V^2}{\Delta V}$$

or

$$H = \sqrt{\frac{2m}{e}}\frac{1}{R}\frac{V}{\sqrt{\Delta V}} = \frac{3.375}{R}\frac{V}{\sqrt{\Delta V}}. \tag{7}$$

For magnetic fields greater than those given by Eq. (7) the loops of the orbit would be too small so that ΔV would not exceed the ionization potential. Therefore, a discharge would not occur. Actually the H values given by Eq. (7) represent a lower limit, somewhat higher values would actually permit a discharge since most electrons have some initial velocity, so that ΔV may actually be somewhat less than the ionization potential. Hence, it may be said that H controls the value of α because if H exceeds the value given by Eq. (7), the number of ionizations per electron per centimeter will be small, i.e., α will be small.

The quantity γ is determined in an important manner by the voltage, since this controls the energy with which the positive ions strike the cathode. Below several hundred volts γ is too small to permit a self-sustaining discharge.

From the foregoing discussion three regions may be outlined wherein a self-sustaining discharge cannot occur. These are as follows:

I. The region below cutoff, where H is less than the value given by Eq. (1). Here no long paths are possible, and hence x is too small.

II. A region of small V, where γ is too small, since the cathode is bombarded by ions of insufficient energy.

III. A region where the magnetic field is too high, so that the path loops are too small to permit the electrons to gain enough energy for efficient ionization. Thus α is too small.

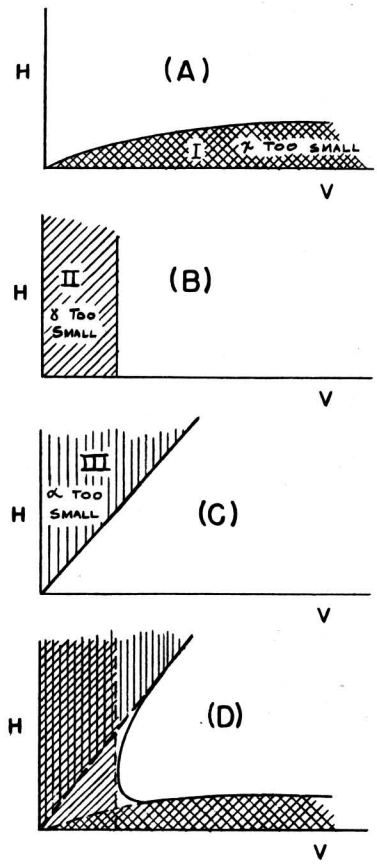

Fig. 12 – Various regions of non-conductivity.

These three regions are shown in Fig. 12a, b, and c, and are combined in Fig. 12d to show the complete characteristic. Experimental curves of this type will be discussed later, and it will be shown that there is fair agreement with most features of the above theory.

Determination of Rectification Criteria

The first tube constructed was a coaxial cylindrical arrangement with a solenoid, as shown in Fig. 4, made to verify previous results. Cutoff curves, as shown in Fig. 3, were obtained by reversing cylinder polarities. It was noticed during rectification tests that the potential of the surrounding solenoid case changed the conducting characteristics of Fig. 3. When the case was grounded, conduction was obtained as usual, when the outer electrode was the cathode, but no conduction was obtained when the center cylinder was the cathode. Placing a wire loop at points B in Fig. 4,

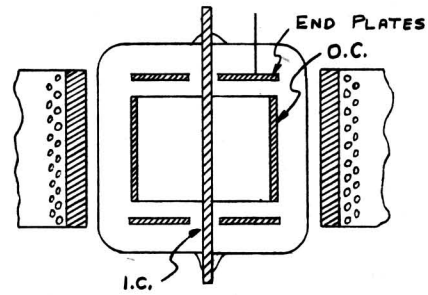

Fig. 13 – Tube for preliminary tests.

reproduced these results. A tube was then constructed with end plates to the cylinders, as shown in Fig. 13. Separate leads were brought out from these end plates, and their potential varied, with respect to the cylinders. A tabulation of the tests made is shown in Table I.

Table I

Electrode Connections for Tube of Fig. 13

Test	Inner Cylinder	Outer Cylinder	End Plates	Conduction
1	Ground	B+	Ground	Yes
2	B+	B+	Ground	Yes
3	B+	Ground	Ground	Yes
4	Ground	B+	B+	No
5	B+	Ground	B+	No
6	Ground	Ground	B+	No

All combinations of electrode potential were tried. It was found that tests No. 1, 2, and 3 showed conduction in the normal manner, whereas tests No. 4, 5, and 6 showed no conduction under any magnetic field, up to the flashover voltage point. These tests indicate that any of the structures of arrangements No. 1, 2, and 3 will rectify. Arrangement No. 5 is the reversal of potentials on 1; 4 the reversal of 3; and 6 the reversal of 2. A sketch of structures based on these arrangements is shown in Fig. 14 with the electrode representing the cathode indicated as K. The letters A, B, and C represent No. 1, 2, and 3 respectively.

These tests indicated that the structure used in the present tube had higher back voltage characteristics than the rectifier of Bush and Smith,[5] due to the presence of two end plates. Also these tests showed the structure of Strutt,[3] as used in a vacuum gauge by Penning,[8] would rectify as in Fig. 14c. The structure of Fig. 14a had not been previously tried as a rectifier. Tests were then made to determine the relative merits of the three structures.

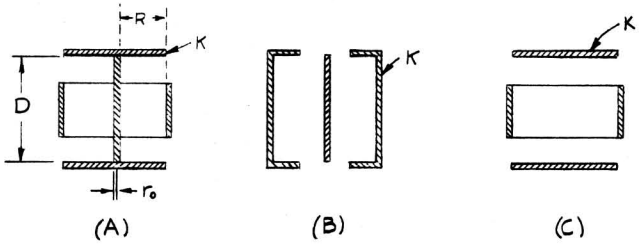

Fig. 14 – Electrode arrangements tested.

In these tests, separate tubes were built, and tests were made at 60 cps. The structure of Fig. 14b was consistently inferior in back voltage to the other two. Thus it was decided to explore various geometries of Figs. 14a and 14c, as a practical rectifier.

DC Characteristics

Two types of d-c characteristics, magnetic cutoff and current-voltage, were taken for different geometries. Three geometrical dimensions were varied, anode radius (R), cathode radius (r_o) and end plate separation (D), as indicated in Fig. 14a. The structure of Fig. 14c was treated as the limiting case of Fig. 14a with zero r_o.

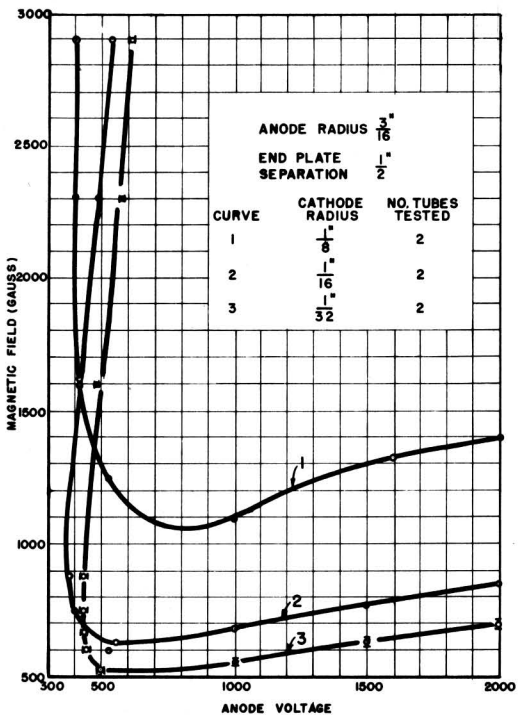

Fig. 15 – Cutoff characteristics.

A. Magnetic Cutoff

A range of anode radii, (R) from 1 inch to 3/32 inch, was used to determine the general variation in cutoff with geometry. Two anode radii (R), 3/16 and 3/32, were then selected in the practical range for a rectifier and their cathode radii (r_o) and end plate separation varied.

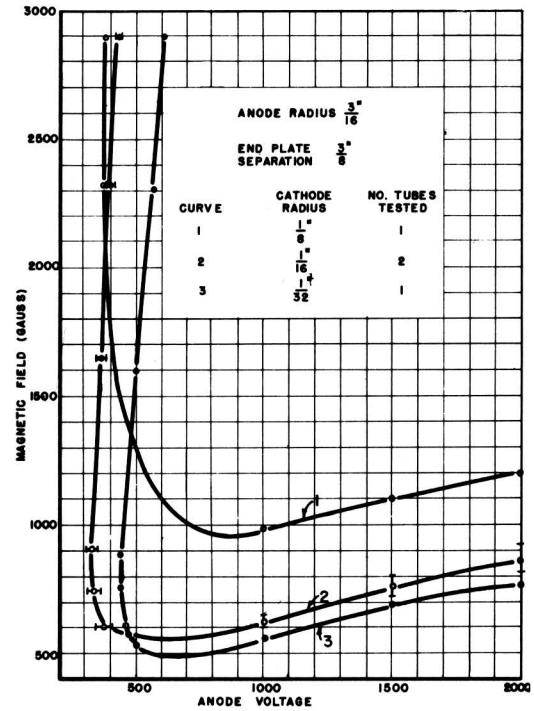

Fig. 16 – Cutoff characteristics.

For the 3/16 inch R, D was made in three dimensions ½ inch, 3/8 inch, and ¼ inch, as shown in Figs. 15, 16, and 17. For each D the r_o was varied three times 1/8 inch, 1/16 inch, and 1/32 inch giving a total of nine variations. An extra curve is plotted in Fig. 17 for the tube with no center pin (Fig. 14c). These curves were taken by noting the voltage across the tube at which current first begins to flow (0.1 μa). For example, it is seen in Fig. 15 that an r_o of 1/8 inch requires a higher magnetic field for conduction than 1/32 inch however, the voltage necessary to start conduction at sufficiently high magnetic fields is less for the 1/8 inch r_o than the 1/16 inch.

The curves for the 3/32 inch R for a D of ½ inch are shown in Fig. 18 for r_o of 1/16, 1/32, and 1/64 inch. The same general variation as in the 3/16 inch R tubes is noted.

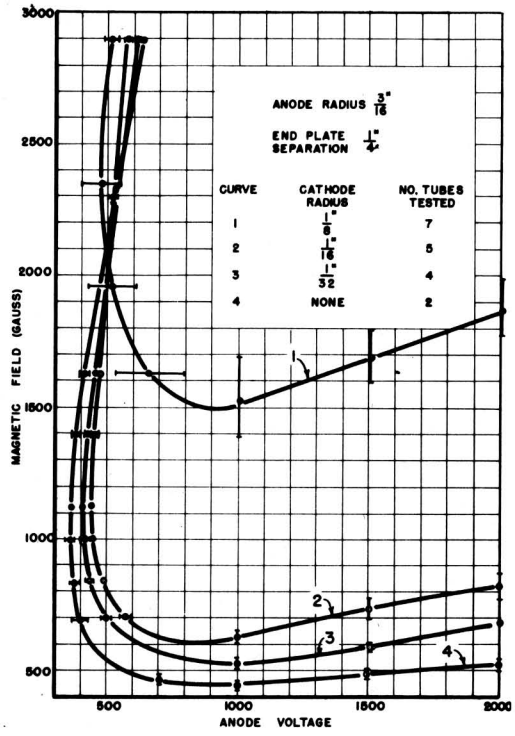

Fig. 17 – Cutoff characteristics.

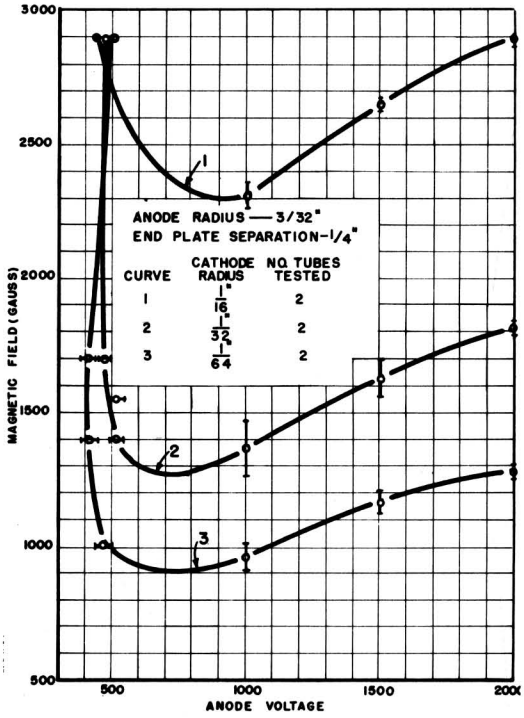

Fig. 18 – Cutoff characteristics.

To explain quantitatively the variation in conduction characteristics with geometry, Eq. (1) may be used. For the case of negligibly small r_o, this equation reduces to

$$H_c = \frac{6.67}{R}\sqrt{V}.$$

The cutoff field at 1000 volts was then selected for the range of tubes with different anode radii and small cathode radii, and plotted in Fig. 19. As the minimum magnetic field occurs near the 1000-volt point, this curve also serves as a guide in predicting the operating field for any desired anode radius.

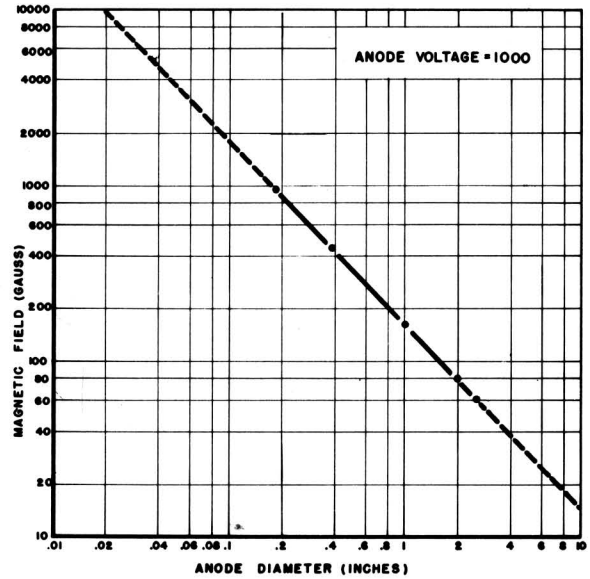

Fig. 19 – Cutoff field as a function of anode diameter.

On the other hand, to check the effect of cathode radius for a particular anode radius, the magnetic field was calculated from Eq. (1) and plotted as a function of r_o in Fig. 20, for the two R, 3/16 and 3/32 inch. It is seen that the tubes with the widest end plate separation (D) approach closest to the theoretical curve. The experimental values are higher than the theoretical probably because electrons originating in the interelectrode space, as well as at the cathode, must be cut off. See Fig. 7 and its discussion. Again these curves can be used to predict the minimum magnetic field for a particular r_o.

B. Current-Voltage

The anode resistances of the tubes were measured at constant magnetic fields by measuring the drop across the tube for currents up to 100 microamps. Higher currents were not used in these preliminary dc tests due to

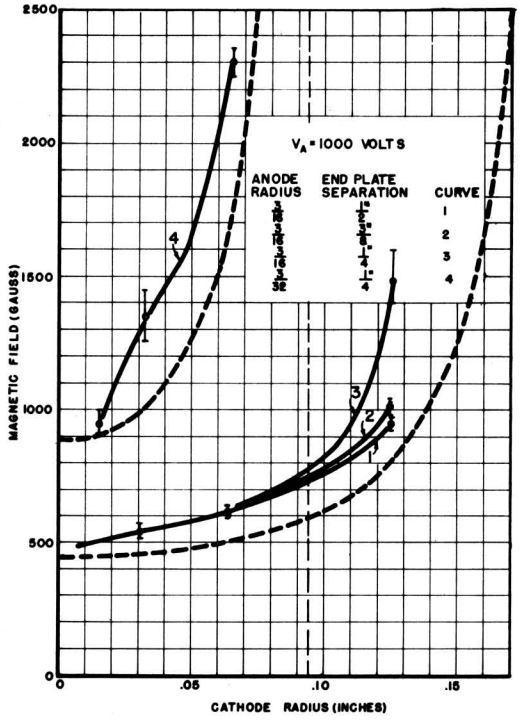

Fig. 20 – Cutoff field as a function of cathode radius.

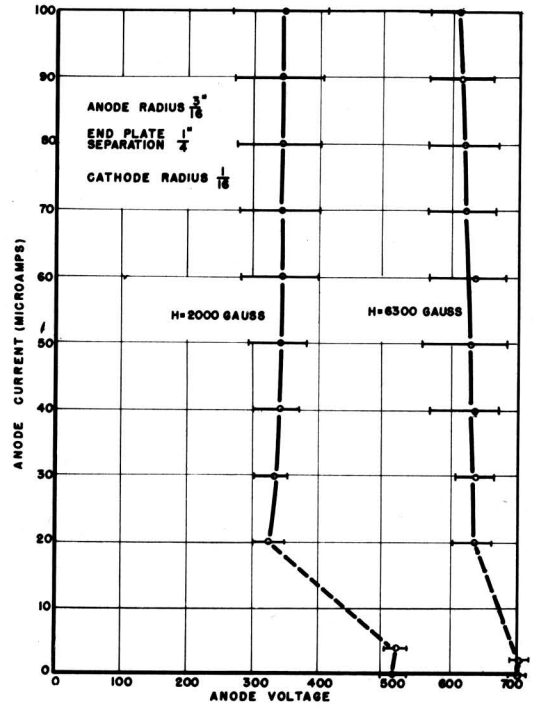

Fig. 22 – Current–voltage curves.

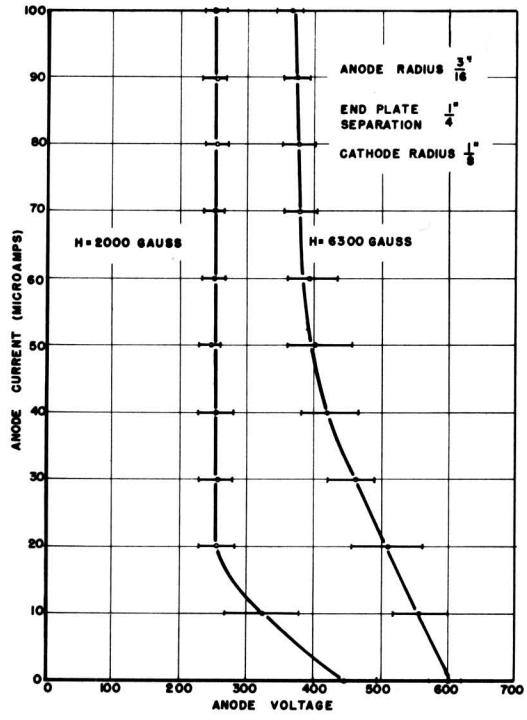

Fig. 21 – Current–voltage curves.

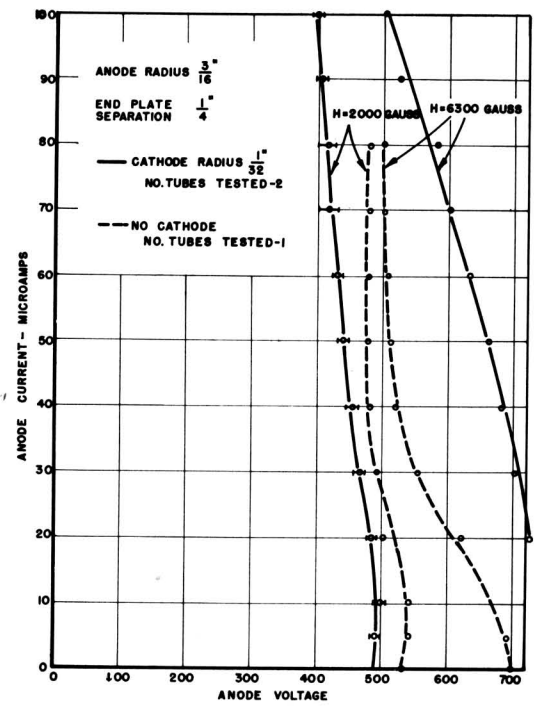

Fig. 23 – Current–voltage curves.

temperature changes arising from the increased power input.

The anode resistance for the structures used in the cutoff curves of Fig. 17 are shown in Fig. 21 for the 1/8 inch r_o, in Fig. 22 for the 1/16 inch r_o, and in Fig. 23 for both the 1/32 inch r_o and the tube with no center pin. In each case the higher tube drop was due to the larger magnetic field (6300 gauss). The resistance curves for the different anode radius (3/32 inch) of Fig. 18 are shown in Fig. 24. These curves follow the same general variation of higher tube drop with smaller center pins and higher magnetic fields.

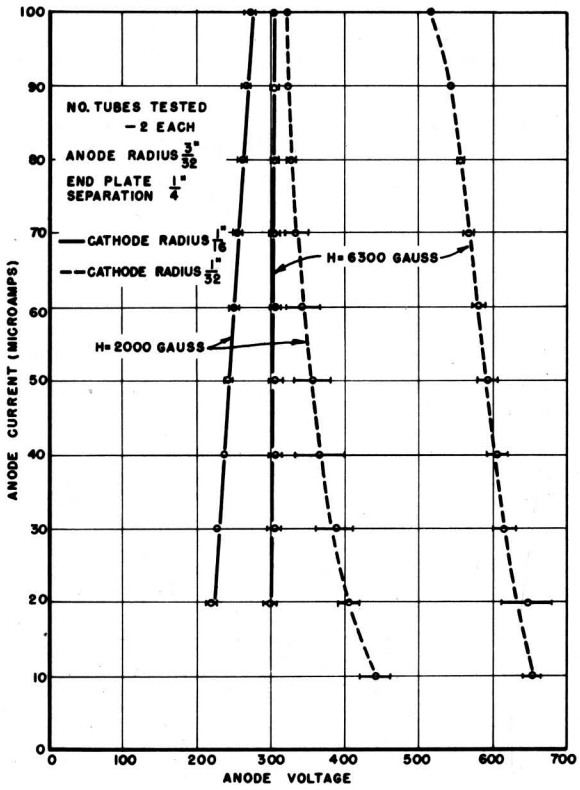

Fig. 24 – Current-voltage curves.

AC Characteristics

The rectification efficiency at different frequencies is a function of two factors, starting time for conduction on the positive cycle, and deionization time, causing conduction on the negative cycle.

A. Starting Time

The time required for the residual charges in the interelectrode space to build up to a steady discharge by cumulative ionization after the anode voltage is applied is termed the starting time. The experimental results are shown in Fig. 25 where the starting time is plotted as a function of the magnetic field for different voltage amplitudes of an applied square pulse. The time was measured by an oscilloscope across a 200-ohm resistance in series with the tube.

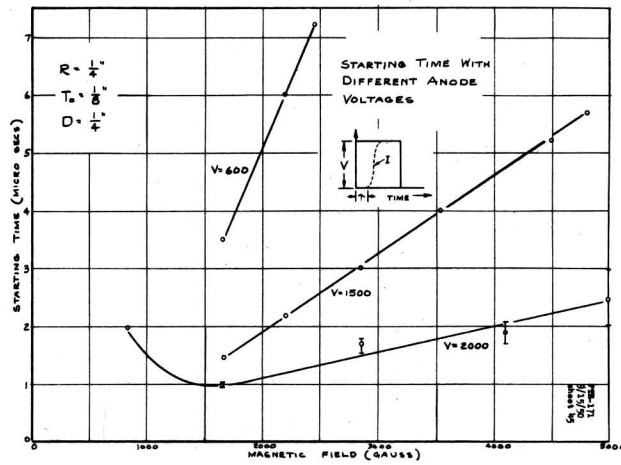

Fig. 25 – Starting time with different anode voltages.

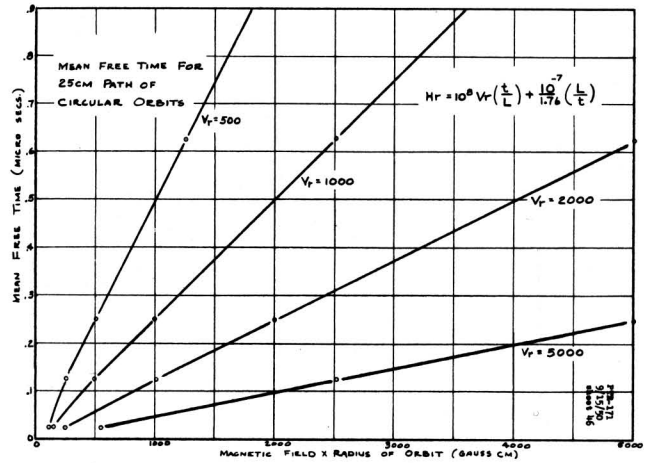

Fig. 26 – Mean free time for 25 cm. path of circular orbits.

To get some theoretical indication of the order of magnitude of the time required for an electron to travel a mean free path, which is approximately 25 cm in mercury vapor at room temperature, stable circular orbits with different initial velocities around the cathode were considered. The mean free time, thus computed, was plotted against the product of the magnetic field H and orbit radius r for different space potential V_r in Fig. 26. The difference between the mean free time and

starting time is presumably due to the ionization build-up time. The starting time of one to two microseconds imposes one frequency limitation.

B. Deionization Time

The second effect, deionization time, was found to be the predominant frequency limitation in the tubes first tested. A tube with $\frac{1}{2}$ inch R operated satisfactorily at 90 kc with neon gas at 10^{-3} mm Hg pressure, but gave no dc output with mercury vapor at the same pressure. Calculations of ambipolar diffusion rates showed the positive ion current would decrease to $\frac{1}{e}$ of the initial value in 0.6 microsecond for neon but would take 11.6 microseconds with mercury vapor. At 90 kc, this diffusion time for mercury is long compared to the duration (of 6 microseconds) of the positive half cycle resulting in positive ions still in the interelectrode space on the negative half cycle. As the decay time varies with the square of the electrode spacing, calculations showed that when R equals to 3/16 inch, the characteristic time is reduced to 2 microseconds. A tube based on these calculations gave satisfactory operation at 90 kc.

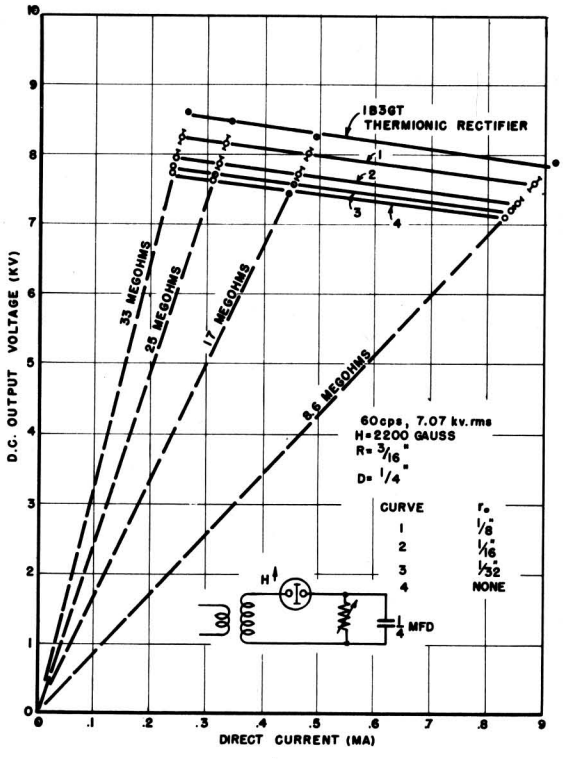

Fig. 27 – Output voltage versus load current.

C. Frequency Characteristics

To determine the rectification efficiency as a function of frequency, the different tubes were tested at 60 cps and then at 90 kc. In the 60 cps tests, the dc currents for four load resistances were measured and the dc voltage calculated. Fig. 27 shows the results of tests on the tubes whose cut-off characteristics are shown in Fig. 17. When compared with the common 1B3GT thermionic rectifier. It is seen that the decrease in dc output voltage, compared to the 1B3GT, corresponds roughly to the starting voltages for the used magnetic field of 220 gauss. Thus, the tubes with the smallest r_o give the lowest output voltages at low frequencies due to higher starting voltages. The effect of geometry, however, at higher frequencies is much more pronounced.

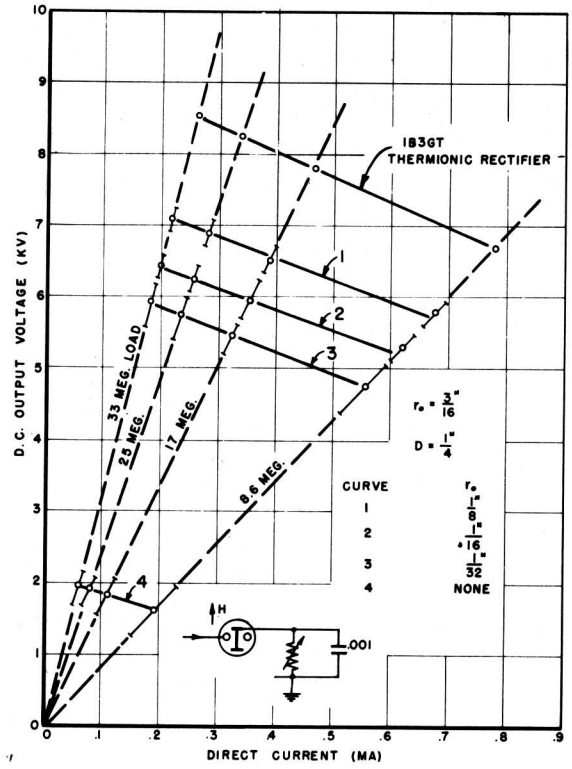

Fig. 28 – Output voltage versus load current.

For the higher frequency tests, the output voltage from a standard RCA 630 TS high-voltage supply was used, the effective frequency being 90 kc. The output currents of the same tubes as shown in Fig. 27, with the same load resistances, are plotted in Fig. 28. The tube drop was then determined by subtracting the output voltage of the particular tube from the output

of the 1B3GT and plotted as a function of the anode cathode spacing in curve 1 of Fig. 29. To determine the high-frequency loss alone, the tube drops due to starting voltage on 60 cps tests of Fig. 27 were subtracted from curve 1 and plotted as curve 2 in Fig. 29. In curve 2 the drop varies as $(R-r_o)^{1.8}$.

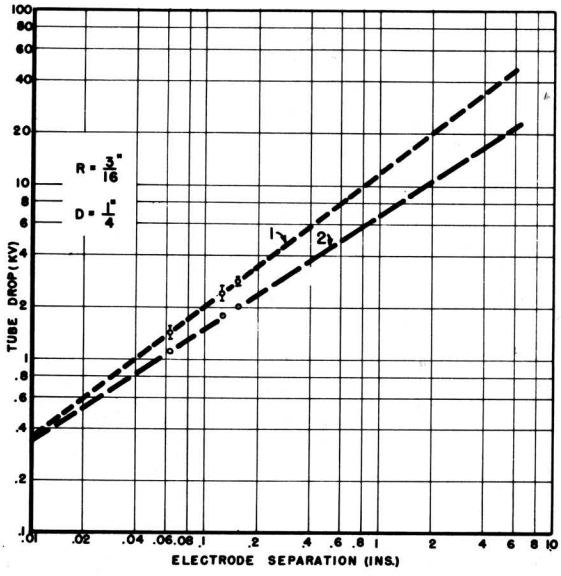

Fig. 29 – Tube voltage drop versus electrode separation.

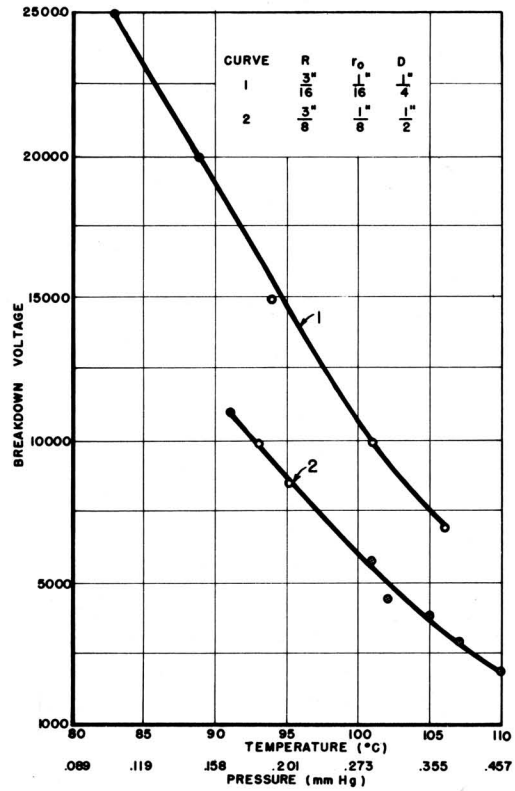

Fig. 30 – Inverse breakdown voltage as a function of temperature and mercury vapor pressure.

Temperature Characteristics

The use of saturated mercury vapor in this rectifier imposes both low and high temperature limits. When the temperature is reduced below room temperature conduction requires a higher magnetic field due to a shift of the cutoff curves upward along the magnetic axis. For example, the minimum magnetic field for curve 2 of Fig. 9 is 1000 gauss at 0 degrees Cent. instead of the 500 gauss at 20 degrees Cent.

At the high temperature end, on the other hand, the peak inverse voltage is reduced due to the increase in pressure. A plot of the peak inverse voltage as a function of temperature (and pressure) is shown in Fig. 30 for two geometries. The larger tube shown in curve 2 breaks down at lower voltages in accordance with Paschen's law. No d-c data were taken above 30 kv; however, at 60 cps, tubes were operated up to 40-kv peak inverse voltage.

Tube Development

The development of the rest of the tube around the basic trapping structure of Fig. 14 was determined by three factors, a high inverse voltage, stability of operation, and long life. The structure was changed four times as illustrated in Fig. 31 to meet these requirements.

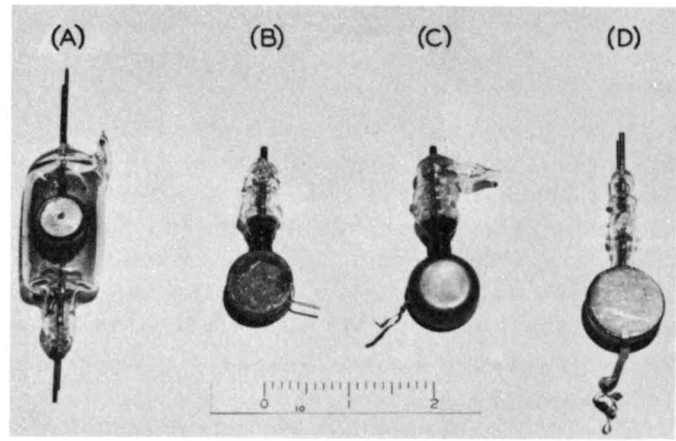

Fig. 31 – Successive modifications of the tube.

In the glass bulb structure of Fig. 31a, the inverse voltage was 25 kv; however, stable operation was only a few hours due to material sputtering from the center pin onto the glass wall.

Next, to shield the glass insulation from sputtering and reduce the volume available for a gas discharge along a long path, the structure was changed to a metal type as shown in Fig. 31b. Here two cold-rolled steel end plates, having a stainless steel center pin, were copper-brazed to a stainless steel cylinder. The anode lead was suspended by a glass insulating tube which was sealed to a Kovar eyelet in the stainless steel cylinder. The sputtering on the glass insulation in this tube was considerably reduced; however, instability was noted after any high current discharges inside the tube. Tests indicated that the pressure was reduced after the discharge due to contamination of the mercury by copper which had been vaporized from the brazed joint. To eliminate one of the copper seals and to make the brazing easier a monel cup with a monel end plate was used, as shown in Fig. 31c, instead of the stainless steel cylinder. Although the brazing was easier, the same instability after heavy discharges was noted. It then appeared advisable to eliminate all metal-to-metal seals.

A metal-glass bulb tube is shown in Fig. 31d, 32, and 33a, where Kovar end plates are attached to a glass cylinder. The glass insulating tube, which supports the anode lead at one end, is sealed to the glass cylinder at the other end. No instability was noticed in this tube after heavy discharges were induced in the tube. Tests were then made to test the actual life of the tube while under peak inverse voltages of 28 kv and $\frac{1}{2}$ ma dc rectified current, at 60 cps.

On life test, this tube operated satisfactorily for 600 hours at which time a sustained discharge began, due to the peeling off of material, which had sputtered from the stainless steel center pin to the end plates. To reduce sputtering, a graphite center pin was substituted for the stainless steel pin.

Life tests on the graphite center pins indicated these tubes would operate for at least 1000 hours; however, after 500 hours sparkovers of a few minutes duration began to occur on the average of one every twenty-four hours. Thus, graphite, although better than stainless steel, was not wholly satisfactory for a practical life.

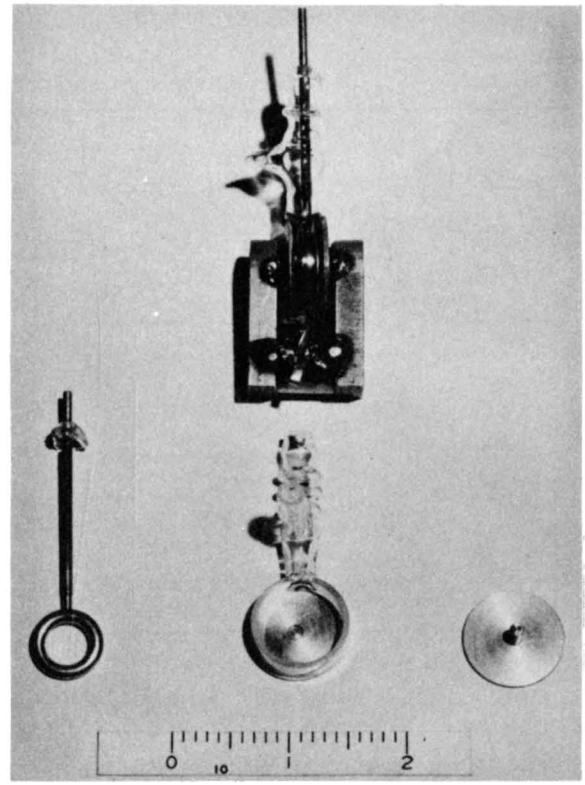

Fig. 32 – Tube assembly and parts.

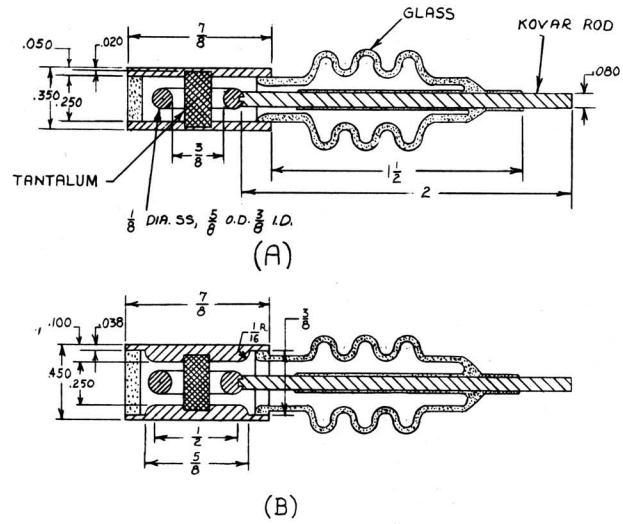

Fig. 33 – Drawings of two modifications of the tube.

In an attempt to further reduce the sputtering, tantalum metal was then tried for the center pin. Sheet tantalum, .0025 inches thick,

was wrapped around a stainless steel center pin and inserted in the tube. On life test, this tube did not flashover a single time until a point discharge started from a loose end at 1200 hours. Examination of the tantalum showed the loss of volume due to sputtering to be at least 1/500 that of the graphite. Recently tubes with solid tantalum pins have been constructed, which have operated up to 3000 hours.

The final change in design was made to increase the distance between the ragged edge of the glass to metal seal from the anode ring by shaping the end plates. A diagram of the tube with flat end plates, of Fig. 31d, is drawn in Fig. 33a as a comparison with the new dished type of end plates of Fig. 33b. Tests showed the field emission from the glass to metal seal in this joint to be considerably reduced.

Ernest G. Linder

Ernest G. Linder

REFERENCES

[1] C.E.S. Phillips, *Proc. Roy. Soc.*, 64, 172 (1898).

[2] C.E.S. Phillips, *Phil. Trans.*, 197A, 135 (1901).

[3] R. J. Strutt, *Proc. Roy. Soc.*, 89A, 68 (1913).

[4] M. Wehrli, *Ann. d. Physik*, 69, 289 (1922).

[5] V. Bush and C.G. Smith, *Proc. I.R.E.*, 10, 41 (1922).

[6] A.W. Hull, *Phys. Rev.*, 18, 31 (1921).

[7] F.M. Penning, *Physica*, 3, 873 (1936).

[8] F.M. Penning, *Physica*, 4, 71 (1937).

[9] See K.R. Spangenberg, Vacuum Tubes, McGraw–Hill (1948) pp. 116 and following.